Supplementary Information

Layer-Dependent Transport and Optoelectronic Property in Two-Dimensional Perovskite: $(PEA)_2PbI_4$

Yu-Qing Zhao[1§], Qi-Rui Ma[1§], Biao Liu[3], Zhuo-Liang Yu[1], Junliang Yang[3], Meng-Qiu Cai[1,2*],

1.School of Physics and electronics Science, Hunan University, Changsha, Hunan 410082, People's Republic of China

2.Synergetic Innovation Center for Quantum Effects and Applications (SICQEA), Hunan Normal University, Changsha 410081, China

3.Hunan Key Laboratory for Super-microstructure and Ultrafast Process, School of Physics and Electronics, Central South University, Changsha 410083, Hunan, China

Table S1 Calculated lattice constants a, b and Δc (the inter layer distance between two adjacent inorganic octahedral PbI_6^- framework) of 2D layered $(PEA)_2PbI_4$ with different thicknesses.

Layers	1	2	3	Bulk	Bulk-exp[1].
a	8.30	8.30	8.34	8.55	8.79
b	8.97	8.98	9.00	9.15	9.39
Δc	14.47	14.37	14.44	14.50	14.42

Table S2 The reported detail data of deformation potential E_1, stretching modulus C_{2D}, effective masses m* and charge carrier mobilities μ for 2D monolayer graphdiyne, phosphorous, MoS2 as well as bulk $MAPbI_3$, Si crystal[2-6] in previous work compared with our work in table 1.

	Carrier type	E_1(eV)	C_{2D}(N/m)	m*(m_0)	τ(ps)	μ($cm^2V^{-1}s^{-1}$)
graphdiyne	e[a]	2.09	158		19.11	208100
	h[a]	6.30	158		1.97	19700
	e[b]	2.19	145		17.22	172200
	h[b]	6.11	145		1.91	19100
phosphorous	e[a]	2.72	29	0.17	0.174	1100

	h^a	2.50	29	1.12	0.126	640
	e^b	7.11	102	0.15	0.112	80
	h^b	0.15	102	6.35	0.067	10000
	e^a	10.88	127	0.46	0.124	77
	h^a	5.29	127	0.57	0.104	200
	e^b	11.36	128	0.48	0.151	60
MoS_2	h^b	5.77	128	0.60	0.069	152
	e			0.21		1500
$MAPbI_3$	h			0.32		800
	e					1350
Si	h					480

Table S3 Calculated effective masses, dielectric constants and exciton binding energy of layered perovskite $(PEA)_2PbI_4$.

	Conduction band				Valence band						
N	m_{xx}	m_{yy}	m_{zz}	$<m_c^*>$	m_{xx}	m_{yy}	m_{zz}	$<m_c^*>$	μ	ε_∞	E_b(meV)
1	0.38	0.76	∞	0.57	0.64	0.67	∞	0.66	0.31	3.93	272

2	0.4	0.54	∞	0.47	0.61	0.60	∞	0.60	0.26	3.93	228
3	0.35	0.45	∞	0.4	0.57	0.59	∞	0.58	0.24	3.93	210
bulk	0.35	0.4	∞	0.38	0.56	0.47	∞	0.52	0.22	3.93	193

Figure S1 Plotted band structures of (a) monolayer, (b) bilayer and (c) trilayer of 2D layered perovskite $(PEA)_2PbI_4$ by employing GGA potential function.

Figure S2 Plotted total and partial density of bilayer perovskite $(PEA)_2PbI_4$. The black line represents total density of states (TDOS). The red line, blue, and pink line represents the electron density states of total Pb atoms, I atoms and partial Pb atoms. Considering the model of bilayer perovskite $(PEA)_2PbI_4$, the density of total Pb atoms represented by red lines change into the partial density indicated by pink lines when removing the Pb atoms of the middle layer. Thus, lead atomic orbital energy increase, indicating that there is mainly lead atomic orbitals of middle layer occupying in the conduction band minimum (CBM). this may be why the band gap becomes larger while bilayer change into monolayer perovskite.

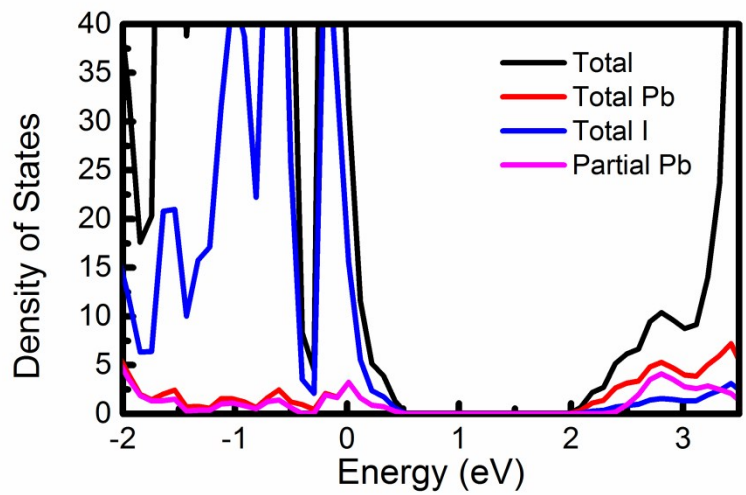

Figure S3 The band edge energy shift of valence band maximum (VBM) and conduction band minimum (VBM) with respect to the lattice dilation along the (a) a direction and (b) b direction for the bilayer perovskite. Solid lines represent the linear fit, which defines DP constants. (c) The total energy as a function of lattice deformation along the a_0 and b_0 directions. Solid lines are the parabola fittings, which give elastic constant.

Figure S4 The band edge positions of valence band maximum (VBM) and conduction band minimum (VBM) with respect to the lattice dilation along the (a) a direction and (b) b direction for the trilayer perovskite. Solid lines represent the linear fit, which defines DP constants. (c) The total energy as a function of lattice deformation along the a_0 and b_0 directions. Solid lines are the parabola fittings, which give elastic constant.

Reference:

1 S. Yang, W. Niu, A. L. Wang, Z. Fan, B. Chen, C. Tan, Q. Lu and H. Zhang, Ultrathin Two‐Dimensional Organic–Inorganic Hybrid Perovskite Nanosheets with Bright, Tunable Photoluminescence and High Stability, *Angew. Chem. Int. Edit.,* 2017, **56**(15), 4252-4255.

2 M. Long, L. Tang, D. Wang, Y. L and Z. Shuai, Electronic structure and carrier mobility in graphdiyne sheet and nanoribbons: theoretical predictions, *ACS Nano,* 2011, **5**(4), 2593-2600.

3 Y. Q. Cai, G. Zhang and Y. W. Zhang, Polarity-reversed robust carrier mobility in monolayer MoS2 nanoribbons, *J. Am. Chem. Soc.,* 2014, **136**(17), 6269-6275.

4 Y. Wang, Y. Zhang, P. Zhang and W. Zhang, High intrinsic carrier mobility and photon absorption in the perovskite CH3NH3PbI3, *Phys. Chem. Chem. Phys.,* 2015, **17**(17), 11516-11520.

5 Y. P. He and G. Galli, Perovskites for Solar Thermoelectric Applications: A First Principle Study of CH3NH3Al3 (A = Pb and Sn), *Chem. Mater.,* 2014, **26**(18), 5394-5400.

6 M. V. Fischetti and S. E. Laux, Band structure, deformation potentials, and carrier mobility in strained Si, Ge, and SiGe alloys, *J. Appl. Phys.,* 1996, **80**(4), 2234-2252.